



HAL
open science

When magnetic chirality gets excited: spin waves in $\text{Ba}_3\text{NbFe}_3\text{Si}_2\text{O}_{14}$

Mickael Loire, Virginie Simonet, Sylvain Petit, Karol Marty, Pierre Bordet,
Pascal Lejay, Jacques Ollivier, Mechthild Enderle, Paul Steffens, Eric
Ressouche, et al.

► **To cite this version:**

Mickael Loire, Virginie Simonet, Sylvain Petit, Karol Marty, Pierre Bordet, et al.. When magnetic chirality gets excited: spin waves in $\text{Ba}_3\text{NbFe}_3\text{Si}_2\text{O}_{14}$. 2010. hal-00524558v1

HAL Id: hal-00524558

<https://hal.science/hal-00524558v1>

Preprint submitted on 8 Oct 2010 (v1), last revised 30 May 2011 (v2)

HAL is a multi-disciplinary open access archive for the deposit and dissemination of scientific research documents, whether they are published or not. The documents may come from teaching and research institutions in France or abroad, or from public or private research centers.

L'archive ouverte pluridisciplinaire **HAL**, est destinée au dépôt et à la diffusion de documents scientifiques de niveau recherche, publiés ou non, émanant des établissements d'enseignement et de recherche français ou étrangers, des laboratoires publics ou privés.

When magnetic chirality gets excited: spin waves in $\text{Ba}_3\text{NbFe}_3\text{Si}_2\text{O}_{14}$

M. Loire,¹ V. Simonet,¹ S. Petit,² K. Marty,^{1,3} P. Bordet,¹ P. Lejay,¹ J. Ollivier,⁴ M. Enderle,⁴ P. Steffens,⁴ E. Ressouche,⁵ A. Zorko,⁶ and R. Ballou^{1,*}

¹*Institut Néel, CNRS & Université Joseph Fourier, BP166, 38042 Grenoble Cedex 9, France*

²*Laboratoire Léon Brillouin, CEA-CNRS, CE-Saclay, F-91191 Gif sur Yvette, France*

³*Oak Ridge National Laboratory, Oak Ridge, Tennessee 37831 USA*

⁴*Institut Laue Langevin, BP156, 38042 Grenoble Cedex 9, France*

⁵*Institut de Nanosciences et Cryogénie, SPSMS/MDN, CEA-Grenoble, 38054 Grenoble Cedex 9, France*

⁶*"Jožef Stefan" Institute, Jamova 39, 1000 Ljubljana, Slovenia*

(Dated: October 11, 2010)

The spin wave excitations emerging from the helically modulated ferrochiral triangular magnetic order in $\text{Ba}_3\text{NbFe}_3\text{Si}_2\text{O}_{14}$ were investigated by neutron scattering on a structurally enantiopure single crystal. The collected spectra are accounted for in the minimal model explaining the magnetic order and its total chirality. It is found out that the spin waves excitations emerging from this order display remarkable properties: (i) spectral asymmetries answerable to the structural chirality and (ii) spin correlations evidencing full chirality of the spin dynamics over the whole energy spectrum.

PACS numbers: 75.25.-j, 75.30.Ds, 75.40.Gb, 75.50.Ee, 78.70.Nx

Ubiquitous in nature, chirality is what distinguishes a phenomenon from its materialization in a mirror [1]. Within a magnet it accounts for the sense of rotation of the magnetic moments along an oriented line, as in a helical arrangement, or on oriented loops, as with the triangular moment configuration on a triangle. The static magnetic helicity and triangular chirality were found out in a pure state in ordered phases [2–4]. Chiral dynamics were also detected in a number of experiments, but as coming into sight from a breaking of time reversal invariance [5–11]. No case of totally chiral spin dynamics, solely and maximally breaking the space inversion symmetry over a whole spectrum, has been reported so far.

A most suited compound for this investigation is the langasite $\text{Ba}_3\text{NbFe}_3\text{Si}_2\text{O}_{14}$. Its magnetic carriers are the ions Fe^{3+} ($S = 5/2$, $L = 0$), distributed over planar triangular lattices of triangles perpendicular to the trigonal c axis. A magnetic order sets up below the Néel temperature $T_N = 27$ K. The magnetic moments within each triangular plane freeze in a same triangular configuration over each triangle. This ferrochiral arrangement is helically modulated along the c axis with the period $1/\tau \approx 7$. A mean-field analysis suggested that 5 exchange interactions are necessary to account for the observed magnetic order, intra-triangular J_1 and inter-triangular J_2 within each triangular plane and 3 inter-plane (J_3, J_4, J_5) connecting each moment of a triangle to the 3 moments of the upper/lower triangles along the c axis [3]. J_3 and J_5 are oppositely twisted around c and of different strength. This reflects the structural chirality, denoted ϵ_T , inherent to the acentric space group P321. $\epsilon_T = -1$ in the structurally left-handed investigated crystal, implying that J_5 dominates over (J_3, J_4). The magnetic order also exhibits a single helicity, denoted ϵ_H , and a single triangular chirality, denoted $\epsilon_H\epsilon_T$ to emphasize the interdependency between the structural

and the two magnetic chiralities [3, 12, 13]. We recall that $\vec{m} \wedge \vec{m}' = m^2 \sin(\tau)\epsilon_H\hat{c}$ for consecutive moments along c and $\vec{m}_1 \wedge \vec{m}_2 + \vec{m}_2 \wedge \vec{m}_3 + \vec{m}_3 \wedge \vec{m}_1 = (3\sqrt{3}/2)m^2\epsilon_H\epsilon_T\hat{c}$ for the moments ($\vec{m}_1, \vec{m}_2, \vec{m}_3$) of an oriented triangle, with ϵ_H and $\epsilon_H\epsilon_T$ equal to $+1(-1)$ for the right(left)-handed sense of rotation. It was proposed that the ultimate single magnetic chirality selection originates from the antisymmetric Dzyaloshinskii-Moriya (DM) exchange interactions [3]. It suffices to consider intra-triangular interactions with the same DM vector along the c axis for the three bonds. This favors in-plane spin components and selects a magnetic triangular chirality $\epsilon_H\epsilon_T$ according to the orientation of the DM vector along c . A single magnetic helicity ϵ_H then is generated, through ϵ_T .

No enough information were available from the static measurements to quantitatively extract the parameters of the model, giving a first motivation to investigate the spin wave dynamics by inelastic neutron scattering. As to get a global overview, the measurements were performed on the time-of-flight spectrometer IN5 at the Institut Laue Langevin on a single crystal in rotation about the zone axis a , set vertical [14]. The incident wavelength was fixed to 4 Å along with a chopper speed of 16000 rpm, yielding an elastic energy resolution $\delta\hbar\omega \simeq 0.1$ meV. Standard corrections and background subtraction were performed. Corrected data were reduced with the Horace suite software [15] to obtain the excitation spectra as functions of wavevectors \vec{Q} and energy transfer $\hbar\omega$.

The next step was to investigate how the chirality of the static order would extend to the dynamics. It was expected that chiral spin dynamics would emerge from an already totally chiral magnetic order. As a matter of fact, the point of utmost interest was to investigate to which extent in energy the single chirality of the magnetic order in $\text{Ba}_3\text{NbFe}_3\text{Si}_2\text{O}_{14}$ would be found unaltered

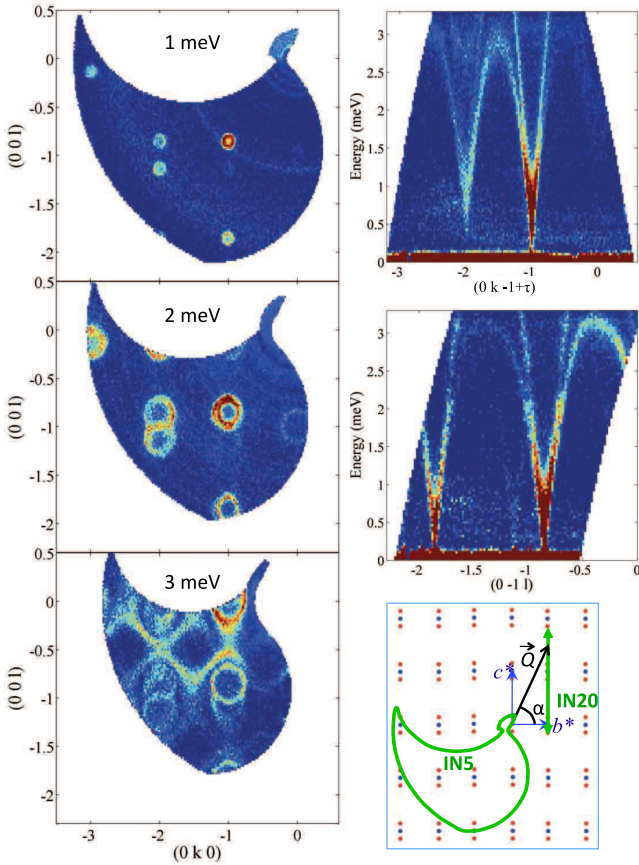


FIG. 1: Inelastic neutron scattering intensities at 1.6 K in the (b^*, c^*) scattering plane on the time-of-flight spectrometer IN5. Displayed are intensity maps at constant transfer energy (energy-cuts) and intensity maps along $(0, k, -\tau)$ and $(0, -1, \ell)$ lines in the reciprocal space (\vec{Q} -cuts). In the bottom right sketch, the green area and arrow show the probed reciprocal vectors on the IN5 and IN20 spectrometers.

in the dynamics. The tool then was inelastic scattering of polarized neutrons with polarization analysis [16, 17]. Although not exclusively, longitudinal polarization analysis in the spin-flip channel along the scattering vector was considered systematically. This consists in polarizing the incident neutron beam along (\uparrow) or oppositely (\downarrow) to the scattering vector \vec{Q} and measuring the intensities $\sigma_{\uparrow\downarrow}$ and $\sigma_{\downarrow\uparrow}$ of the scattered neutrons with the opposite polarization. $\sigma_{\uparrow\downarrow}$ is proportional to $S(\vec{Q}, \omega) + C(\vec{Q}, \omega)$ and $\sigma_{\downarrow\uparrow}$ to $S(\vec{Q}, \omega) - C(\vec{Q}, \omega)$, where $S(\vec{Q}, \omega) = \frac{1}{2\pi\hbar} \int \langle M_y(\vec{Q}, 0)M_y(-\vec{Q}, t) + M_z(\vec{Q}, 0)M_z(-\vec{Q}, t) \rangle e^{-i\omega t} dt$ is the dynamical structure factor, and $C(\vec{Q}, \omega) = \frac{1}{2\pi\hbar} \int \langle M_y(\vec{Q}, 0)M_y(-\vec{Q}, t) - M_z(\vec{Q}, 0)M_z(-\vec{Q}, t) \rangle e^{-i\omega t} dt$ is dubbed chiral magnetic scattering. $M_{y,z}(\vec{Q}, t)$ are the Fourier transform of the components of the moments perpendicular to the scattering vector \vec{Q} in the scattering plane (y) or perpendicular to this (z) at time t . The measurements were performed on the triple-axis spectrometer

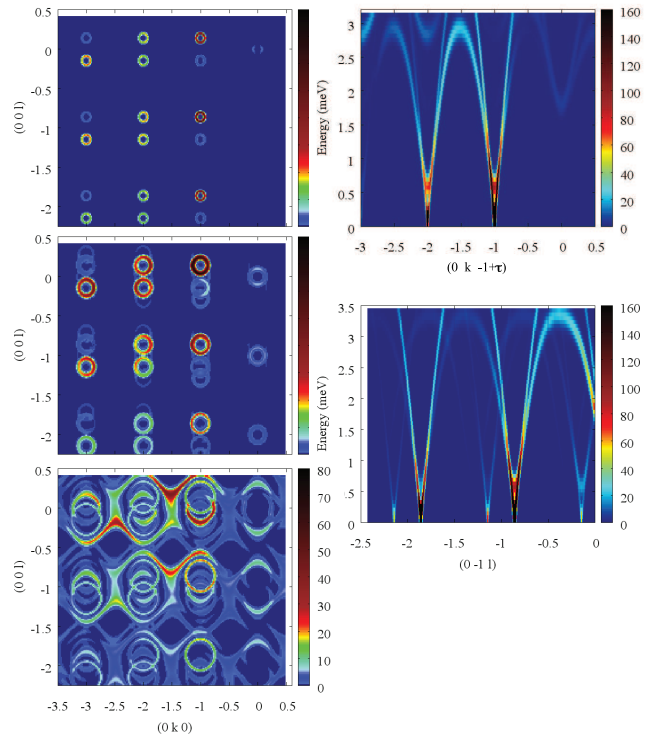


FIG. 2: Dynamical structure factor calculated in the linear approximation from the minimal model of the interactions (see text) to compare with the measurements of Fig. 1.

IN20 at the Institut Laue Langevin, with a fixed final energy of 14.7 meV and an energy resolution of ≈ 1 meV. $S(\vec{Q}, \omega) = (\sigma_{\uparrow\downarrow} + \sigma_{\downarrow\uparrow})/2$ and $C(\vec{Q}, \omega) = (\sigma_{\uparrow\downarrow} - \sigma_{\downarrow\uparrow})/2$ were extracted from the measured $\sigma_{\uparrow\downarrow}$ and $\sigma_{\downarrow\uparrow}$. $S(\vec{Q}, \omega)$ was corrected from the background by subtracting the non spin-flip part, which is valid above 1.5 meV as checked by spherical polarization analysis on selected (\vec{Q}, ω) points. We used CRYOPAD [18] to allow for spherical polarization analysis and to perform the longitudinal polarization analysis in a strictly zero magnetic field environment on the crystal so as to probe the dynamical chirality as arising from the sole space inversion symmetry breaking.

Fig. 1 summarizes our results obtained by inelastic unpolarized neutron scattering. Two spin wave branches emerging from the $\pm\tau$ magnetic satellites can be easily identified. A striking result is the difference between their relative intensities, which strongly depends on the reciprocal lattice node. This is a signature of the crystal non-centrosymmetry. These branches form delicate arches, with different maximum energies (lower branch clearly visible on IN5, maximum of the upper branch only observable on IN20). One of the branch is gapped with a minimum at around 0.4 meV. The other branch could be ungapped at least within the resolution associated with the spectrometer set up (0.1 meV). Less intense modes are also discernible dispersing from the nodes of

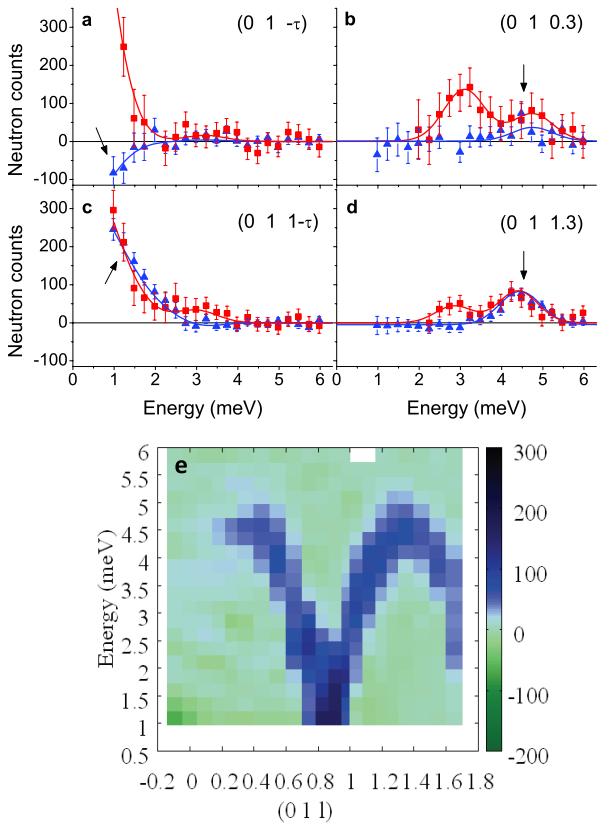


FIG. 3: (a-d) Magnetic scattering $S(\vec{Q}, \omega)$ (red) and chiral contribution $C(\vec{Q}, \omega)$ (blue) as a function of the transfer energy ω at selected scattering wavevectors $(0, 1, \ell)$, extracted at 1.5 K by longitudinal neutron polarimetry on the triple-axis spectrometer IN20. (e) dispersion of $C(\vec{Q}, \omega)$ obtained by gathering the measurements at all ℓ . The spectral weight is only significant for the branch emerging from the $-\tau$ magnetic satellite of the reciprocal lattice node $(0, 1, 1)$. No branch is detected emerging from the other $+\tau$ magnetic satellite.

the reciprocal lattice and associated to the global spin rotational invariance (especially visible along the line at $k = 0$ in the energy-cut at $\omega = 2$ meV) and from $\pm 2\tau$.

To get further insights, zero temperature spin wave excitation spectra were computed, within the standard Holstein-Primakov formalism in the linear approximation [19], considering the minimal model, involving the 5 exchange interactions (J_1, J_2, J_3, J_4, J_5) and an intra-triangular DM interaction. Together with the spin wave dispersion and spectral weights, all the dynamical spin-spin correlation functions were calculated. A thorough comparison of figures 1 and 2 indicates that a good agreement between experiment and calculation is achieved with the exchange parameters $J_1 = 0.85 \pm 0.1$, $J_2 = 0.24 \pm 0.05$, $J_3 = 0.053 \pm 0.03$, $J_4 = 0.017$ and $J_5 = 0.24 \pm 0.05$ in meV. These were constrained to ful-

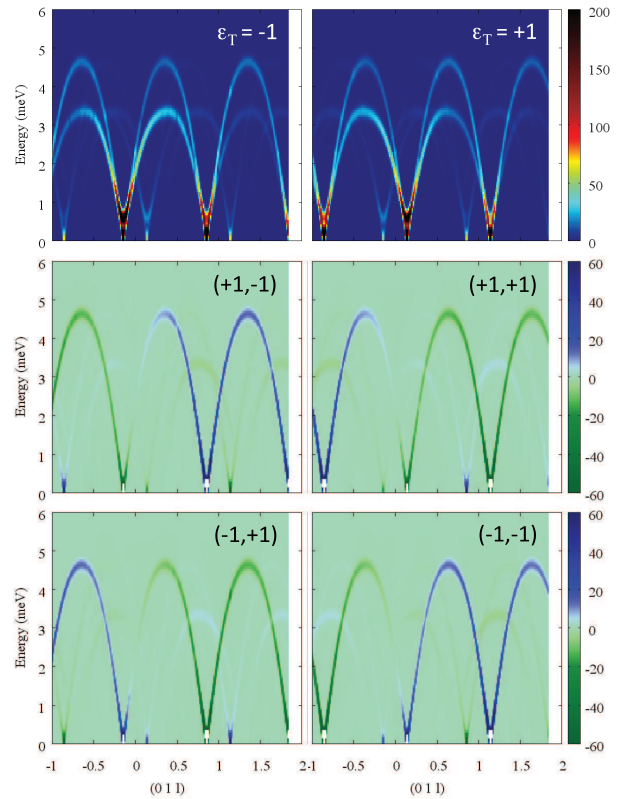


FIG. 4: Computed magnetic scattering for the two structural chiralities $\epsilon_T \pm 1$ and computed chiral contribution for the 4 possible magnetic ground states ($\epsilon_H, \epsilon_H \epsilon_T$). The $(+1, -1)$ calculation compares well with the experiment in Fig. 3

fill the $\tau = 1/7$ and $\epsilon_T = -1$ conditions, and yield a Curie-Weiss temperature of 191 K, in agreement with the susceptibility measurements [3]. The DM vector along the c axis with a positive value of $\approx 1\%J_1$ accounts for the lower branch gap and selects $\epsilon_H \epsilon_T = -1$. A magnetocrystalline anisotropy of $\approx 1\%J_1$ can produce a similar gap, but would not explain the triangular chirality selection. A component of the intra-triangular DM vector along the bond connecting two spins is also allowed [20], whose finiteness is witnessed in electron spin resonance linewidth anisotropy, but is not of basic relevance in the neutron data interpretation. All features of the dispersions and spectral weights of the spin waves are well captured with this minimal model. Additionally, the upper branch is identified as involving correlations between spins components within the triangular plane and is associated to the broken translational symmetry [21]. The lower branch implies correlations between the spin components along the c -axis. Spin waves in $\text{Ba}_3\text{NbFe}_3\text{Si}_2\text{O}_{14}$ have been probed recently also by Stock *et al.* [22], but their model led them to a different interpretation.

Figure 3 gathers our polarized neutrons scattering ex-

periments. Energy-scans were performed for different ℓ values along $(0, 1, \ell)$ with ℓ ranging from $-\tau$ to 1.7 (see sketch in Fig. 1). The magnetic scattering $S(\vec{Q}, \omega)$ (in red in selected scans of Figs. 3a-d) confirms the magnetic origin of the two intense modes, although they are not as well separated as on IN5, due to the lower resolution. By extracting the chiral contribution $C(\vec{Q}, \omega)$ (in blue), it is found that the lower mode is achiral, as a consequence of the one-dimensional spin component involved in the cross product, while in contrast, the upper mode is chiral (see Fig. 3d and e). For this mode, we observe that $C(\vec{Q}, \omega)$ has a tendency to become negative for negative ℓ (compare Fig. 3a and c at low energy). It equals the amplitude of the pure magnetic scattering $S(\vec{Q}, \omega)$ at large ℓ values (see Fig. 3d). The chiral scattering is related to the magnetic chirality up to a geometric factor as shown by a simple calculation of the static magnetic and chiral scatterings for helices with moments lying in the (a, b) plane. Defining α as the angle between the b^* axis and the scattering vector \vec{Q} (see sketch in Fig. 1), the chiral scattering is equal to $\mp \epsilon_H \sin \alpha (m^2/2) |T|^2$ for the $\pm\tau$ satellites respectively, where T is a scalar including phase factors related to the propagation and the different Bravais lattices. The magnetic scattering equals $(1 + \sin^2 \alpha)(m^2/4) |T|^2$. For the case $\epsilon_H = +1$ and $-\tau$ satellite, the sign of $C(\vec{Q}, \omega)$ follows the sign of α , and it equals the magnetic scattering at $\alpha = \pi/2$ which is asymptotically approached for the largest ℓ values in the experiment. This last result points at a full chirality of the upper branch without chirality mixing in the experiment. The dynamical chiral correlation function $C(\vec{Q}, \omega)$ was computed from the model described before. The absence of chirality of the lower branch and the full chirality of the upper branch are confirmed (solution $(+1, -1)$ of Fig. 4). It is observed that, whereas the magnetic scattering differs in spectral weight for the two structural chiralities ($\epsilon_T = \pm 1$), the spin wave chiral scattering is distinct for the 4 magnetic chiralities ($\epsilon_H = \pm 1, \epsilon_H \epsilon_T = \pm 1$) of the underlying magnetic order (see Fig. 4).

In short, the spin waves excitation modes emerging from the totally chiral magnetic order in a structurally enantiopure single crystal of $\text{Ba}_3\text{NbFe}_3\text{Si}_2\text{O}_{14}$ are extremely unusual. As a fingerprint of the crystal chirality and inherent to an exchange twisting, the spectral asymmetry evidenced by inelastic unpolarized neutron scattering already is scarcely offered to observation. The results of inelastic polarized neutron scattering added considerable novelty, owing to the discovery that the spin waves with in-plane correlations are fully chiral at all energy. We recall that the experiments were performed at the base temperature of 1.5 K, of the order of the energy associated with the DM interactions (selecting the chirality of the underlying static magnetic order) and that the neutron energy exciting the system scales in between the DM and the exchange energies (given by the Curie-

Weiss temperature). The absence of chirality mixing of the spin dynamics even at the maximum of the dispersion branches (≈ 4.8 meV) suggests that the spin excitations would practically never reverse the triangular chirality of the magnetic order. This signals very few inelastic collisions of spin waves, indirectly validating the linear spin wave approximation at this temperature. It finally will be heavily emphasized that the crystal was in a strictly zero magnetic field environment (even the earth magnetic field is excluded from it). The experiment thus makes up the first observation of a dynamical chirality unbiased by time-reversal symmetry breaking, namely explicitly and solely associated with the parity breaking.

This work was financially supported by the ANR 06-BLAN-01871. We would like to thank B. Canals and A. Ralko for fruitful discussions.

* rafik.ballou@grenoble.cnrs.fr

- [1] G. H. Wagnière, *On Chirality and the Universal Asymmetry*, WileyVCH, Zürich, Weinheim, 2007.
- [2] M. Ishida, Ya. Endoh, S. Mitsuda, *et al.*, J. Phys. Soc. Jap. **54**, 2975 (1985).
- [3] K. Marty, V. Simonet, P. Bordet, *et al.*, Phys. Rev. Lett. **101**, 247201 (2008).
- [4] M. Janoschek, P. Fischer, J. Schefer, *et al.*, Phys. Rev. B **81**, 094429 (2010).
- [5] B. Roessli, P. Böni, W.E. Fischer, Y. Endoh, Phys. Rev. Lett. **88**, 237204 (2002).
- [6] D. Grohol, K. Matan, J.-H. Cho, *et. al.* Nature Materials **4**, 323 (2005).
- [7] V. P. Plakhty, J. Wosnitza, J. Kulda, *et. al.*, Physica B **385**, 288 (2006).
- [8] H. Braun, J. Kulda, B. Roessli, *et. al.*, Nature Physics, **1**, 159 (2005).
- [9] R. M. Moon, T. Riste and W.C. Koehler Phys. Rev. **181**, 920 (1969).
- [10] S. W. Lovesey and G. I. Watson, J. Phys.: Condens. Matter **10**, 6761 (1998)
- [11] A. Gukasov, Physica B **267**, 97 (1999).
- [12] K. Marty, V. Simonet, P. Bordet, *et al.*, J. Magn. Magn. Mat. **321**, 1778 (2008).
- [13] K. Marty, V. Simonet, P. Bordet, *et al.*, Phys. Rev. B **81**, 054416 (2010).
- [14] J. Ollivier, H. Mutka, L. Didier, Neutron News **21** (2010) 22.
- [15] T.G. Perring, R.A. Ewings, J.V. Duijn, A. Buts, (2009) unpublished, <http://horace.isis.rl.ac.uk/>
- [16] M. Blume, Phys. Rev. **130**, 1670 (1963).
- [17] S. V. Maleyev, V. G. Bar'yakhtar, and R. A. Suris, Fiz. Tverd. Tela **4**, 3461 (1962).
- [18] F. Tasset, Physica B 156-157, 627 (1990)
- [19] T. Holstein, and H. Primakoff, Phys. Rev. **58**, 1098 (1940).
- [20] T. Moriya, Phys. Rev. **120**, 91 (1960)
- [21] D. Belitz, T. R. Kirkpatrick, and A. Rosch, Phys. Rev. B **73**, 054431 (2006).
- [22] C. Stock, L.C. Chapon, A. Schneidewind, *et al.* arXiv:1007.4216.